62-76.docx

Geospatial Analysis of Mass Wasting Susceptibility in Siwalik Region; A Case of Nawalparasi (Bardaghat Susta West), Nepal

Prakash Tiwari
Golden Gate International College, Tribhuvan University, Kathmandu, Nepal

Keywords
Mass-wasting, Susceptibility, Frequency ratio model, Area under curve

Received: 6 September 2025
Revised: 5 Octomber 2025
Accepted: 3 December 2025

ISSN: 3059 - 9687

Abstract

Siwalik hills are occupied in the southern Himalayas and connect to Nepal's southernmost Terai bounded by Main Frontal Thrust in the south and the Main Boundary Thrust in the north. Landslides, Debris flow and Erosion are Mass-wasting phenomena that remobilize sediments deposited on weak and brittle Siwalik hill slopes. This study aims to analyze mass wasting phenomena and prepare Mass-wasting susceptibility map by using frequency ratio model. Total 680 polygon of mass waste incident were recognized from Google earth and by field investigation. Study area cover 250 sq. km, out of which mass waste incidents cover 7.24 sq. km (2.89%). Landslide, Debris flow and Erosion contributes 36.60%, 57.04% and 6.36% respectively to total mass waste incidents. Susceptibility map was categorized into five classes as very low, low, medium, high and very high class covered 42.38%, 28.52%, 22.94%, 4.19% and 1.95% respectively. Performance of model was evaluated using area under curve (AUC). Success rate curve showed 82.15 % and prediction rate curve showed 78.30 % of the area lying under the curve. Mass-wasting susceptibility maps can be used as a planning tool by prioritizing areas for controlling the mass waste effects. District boundary has been selected for this study so that district individually can implement action plan may reduce coordination issues.

1. Introduction

Mass-wasting is natural phenomena occurs when rock, dirt, or debris moves downward due to gravity's effect. Throughout human history, mass-wasting has been a typical phenomenon (Larsen & Parks, 1997). Every year, landslides and mass movements occur in Nepal's Himalayas (Upreti, 1999). The Himalayas are an area with a complicated combination of mass-wasting factors and one of the world's highest rates of mass-wasting (Froude & Petley, 2018). The degree and type of movement are determined by a number of geological, environmental, geomorphological, and hydrologic factors, as well as some additional environmental stress factors, including biotic factors (Cao et al., 2019).

Aside from the loss of life and property, mass waste has a negative impact on the Himalaya ecosystems and add a significant amount of sediment to streams and rivers (Regmi, 2014). Siwalik hills are occupied in the southern Himalayas and connect to Nepal's southernmost Terai (Indo-Gangetic plain) bounded by two major geological structures: The Main Frontal Thrust (MFT) in the south and the Main Boundary Thrust (MBT) in the north. The geology of the Siwaliks is divided into three geological units: Lower Siwalik, Middle Siwalik, and Upper Siwalik (Auden, 1935; Hagen, 1969; Chaudhari, 1982; Dhakal, 2015). Due to weak geological condition and adverse lithostratigraphic situation, trends of mass-wasting phenomena are increasing day by day in Siwaliks region (Bhandari & Dhakal, 2018).

For several mass-wasting hazard susceptibility models, RS and GIS methodologies have been used (Zinck et al., 2001; Akgun et al., 2012; Rowden & Aly, 2018). The use of RS and GIS has grown significantly in response to the need for faster data collection and better mass-wasting bitmaps for commercial satell[illegible]ts. Furthermore, GIS is a useful tool for studying multidimensional events (Cao et al., 2019). It is critical that the input parameters preserve their spatial correlations in order to generate reliable outputs from these models (El Morjani et al., 2007)

Siwalik region (Churiya region) spread over 37 districts in Nepal from East Ilam to West Kanchanpur and covers 12.78 percent of the total land area (President Chure Terai Madhesh Conservation Development Board). In the Siwalik region, multiple landslides and debris flows occur due to an active thrust and continual erosion of material from the surface during the rainy season (Bhandari & Dhakal, 2019a). The erosion of the Chure hills has an adverse effect on communities and settlements downstream. Year after year, a great number of major and small landslides occur in this region, especially in the steep areas, threatening both cultivable lands and human settlements (Singh, 2010). The topography of Siwalik region of 'Nawalparasi (Bardaghat Susta West)' is made up of steep slopes and is divided into three sections: Lower, Middle, and Upper Middle Siwalik.

Many researchers have studied the Siwalik zone's landslides (Ghimire,2010; Devkota et al., 2013; Regmi et al., 2014; TU-CDES, 2017; Bhandari & Dhakal, 2018; Bhandari & Dhakal, 2020), Debris Flow (Bhandari & Dhakal, 2019a; Bhandari & Dhakal, 2019b) and Erosion (Lague & Davy, 2003) in the past. But there is lack of brief quantitative comparative linguistics of three fundamental process together and common factors associated with them. During monsoon period, all the river catchment is in spate with bank-full discharges and cause flooding and inundation in ''Nawalparasi (Bardaghat Susta West)'. Landslides and debris mass obstruct the route of Siwalik villages connection. Every monsoon season, Flash flood with high sediment load posing a transportation issue in East-West highway. Political (District) boundary has been selected for this study so that local body and related stakeholders can implement their action plan independently may reduce coordination issues. Plantation programs can be specified to susceptible area.

2 Materials and Methods

2.1 Study Area

Study area lies in Siwalik region of the 'Nawalparasi (Bardaghat Susta West) (Nawalparasi west of Bardaghat Susta). It is one of 37 chure districts. 'Nawalparasi (Bardaghat Susta West) is a district located in Lumbini Province of Nepal covers about 774.05 sq. Km area. The district is bordered on the east by Nawalpur,

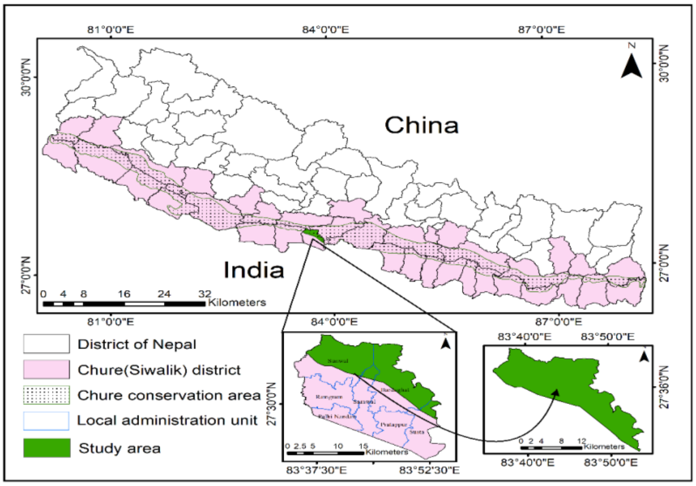

Figure 1: Location map of study areas

on the west by Rupandehi, on the north by Palpa and Tanahu and on the south by the allied states of Uttar Pradesh and Bihar. Study area covers whole Siwalik region of the district include two municipality Sunwal & Bardhaghat and two rural municipality Sarawal & Susta of the northern part. Total area covered by study area is 250 sq. km ranges from latitudes N27˚27'30" and N27˚41'30" to longitudes E83˚36'0" and E83˚54'0"(Fig.1).

The study site lies in tropical and subtropical climate where the rainy season begins in June and ends in September. It has a minimum temperature of 5 degrees Celsius and a maximum of 44 degrees Celsius. Major rivers of this area are Turiya, Jharahi and Dhanewa. The study area covers whole Siwalik region of 'Nawalparasi (Bardaghat Susta West) and some part of Terai as well. Siwalik region of this area include both hills, bhabar and small valley(duns). Only part of terai up to where debris mass is deposited induced from Siwalik region is taken. The topography fluctuates from gentle to steep, and there is also a pressure ridge can be seen.

2.2 Methods of Data Collection

Mass waste occurs in a variety of shapes, sizes, and speeds (Cao et al., 2019). Processes of Mass-wasting phenomena in study area were identified by frequent field visits and satellite images along with expert judgements. Mass-wasting accelerated mainly through three processes: Landslide, Debris flow and Erosion. The distribution and characteristics of mass-wasting in the study area can be seen using an inventory map (Yalcin et al., 2011). Thus, to fulfill main objectives of the study, inventory map was prepared and influenced factors were identified. Both primary and secondary sources of data were collected to prepare the spatial inventory map and various thematic layer of influence factors.

2.2.1 Primary Data Collection

Primary data was gathered through field observation using devices such as a GPS and a checklist. Frequent field surveys were conducted to obtain data for study purpose. Field survey focused on geospatial parameter that influence the Mass-wasting.

2.2.2 Secondary Data Collection

Secondary data was compiled from a variety of sources. The topographical features and related information of the research region were studied using topo-sheet number 099-14 Sunwal,105-03 Bardaghat and 105-08 Tribeni with a map scale of 1:25,000 collected from Department of survey (DoS), Government of Nepal. Google Earth Imagery was utilized to indicate the mass waste polygon. It was also used to draw the validated polygon of mass waste and conduct additional investigation. Geological map of scale 1:250000 was used to study the geological condition of area of interest collected from Department of Mines and Geology, Government of Nepal. Different Influence factor (Slope, Aspect, Curvature, Elevation, Hillshade, Topographic wetness index, Sediment transport index and Stream channel) map were prepared from DEM downloaded from Alaska satellite facility, Road network by editing open street map with the help of google earth and land use/cover map provided by Esri, 2020 land cover map at 10m resolution.

2.3 Mass-wasting Inventory

Mass-wasting (Landslide, Debris Flow, Erosion) inventory map were prepared using Google earth pro2021. The mass waste inventory was updated remotely using visual interpretation and digitalization of mass waste taken on Google Earth satellite images from 2004 to 2021 (February 2021). Inventory was prepared by using polygon-based method. From scar to toe, polygons were drawn to form landslide and Erosion inventory map. Following the flow channel, the polygons were drawn from scar to fan to form Debris flow inventory map. A total 680 polygons were identified and mapped out of which 352 are landslide, 306 are erosion and 22 are Debris flow channel polygon.

2.4 Susceptibility mapping

For geospatial Mass-wasting analysis, it requires base map and factor map. Mass waste Inventory map was used as a Base map. Based on effectiveness and availability factors were selected. Selection of factors totally based upon previous research and frequent field visit. For this research slope, aspect, curvature, elevation, hillshade, topographic wetness index, sediment transport index, geology, distance from road and streams, land cover and soil type were considered as major influencing factors. Total 11 factors were taken. All of these factors were utilized to create various factor maps. The Mass-wasting geospatial analysis was done using these factors maps and base maps in ArcGIS and Microsoft Excel.

By using GIS, polygon created in google earth exported in ArcGIS 10.8 with ‘Kml to layer’ tool. Area and perimeter calculated in the projected coordinate system WGS 1984 44N. All Mass-wasting polygon were merge by ‘geoprocessing tool’. Then combine mass waste polygon 680 polygon divided into train mass waste 510 polygon (75%) and test mass waste 170 polygon (25%) by ‘geostatistical analyst tool’.

These polygon shapfile converted to raster format by ‘Features to raster’ conversion tool. Factors map like Slope, Aspect, Curvature, Elevation, Hillshade, Topographic wetness index (TWI), Sediment transport index (STI) and Distance from stream were prepared by using Digital Elevation Model (DEM) (Figure 2(a-h)). Distance from Road map was prepared by using Open Street Map (Figure2(i). Geological map was prepared by Geological map provided by Department of Mines and Geology, Government of Nepal of scale 1:250000 (Figure2(j). Land use/land cover map was prepared by using Esri 2020 landcover image at 10m resolution (Figure2(k).

TWI and STI were calculated by using following equation (Equation 1 & 2).

$$TWI = Ln\left(\frac{As}{tan\beta}\right) \qquad (1)$$

$$STI = \left(\frac{As}{22.13}\right)^{0.6} * \left(\frac{sin\beta}{0.0896}\right)^{1.3} \qquad (2)$$

Where, As is the specific catchment area (m^2 /m) and β (radians) is the slope (in degrees) (Regmi et al., 2014).

The topographic wetness index (TWI) measures soil moisture and surface saturation and assesses the impact of local topography on hydrological processes. It measures the quantity of water that has accumulated in a watershed and its capacity to flow downward under gravity (Gokceoglu et al., 2005). Erosional and depositional process of a stream is characterized by the sediment transport index (STI) (Regmi et al., 2014).

Each factors map was reclassified based on previous research work and then cross tabulate with train mass waste through ‘Cross tabulation’ tool. Tabulate data exported to Microsoft Excel to analyze geospatial condition of the study area. Frequency ratio model applied. The steps for calculating a FR for a class of landslide-influencing factors are listed below (in Equation 3) (Lee & Pradhan, 2007).

$$FR = (A/B)/(C/D) \qquad (3)$$

Where A represents the number of pixels with mass waste for each factor, B represents the total number of mass waste in the study area, C represents the number of pixels in the factor's class area, D represents the total number of pixels in the study area, and FR represents the frequency ratio of a class for the factor.

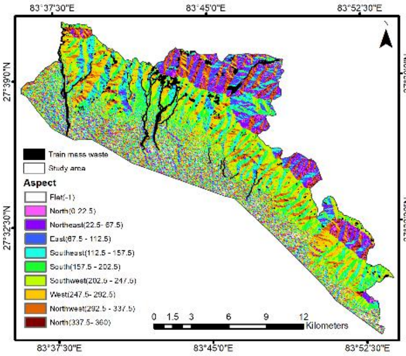

(a) (b) (c)

(i)

(d) (e)

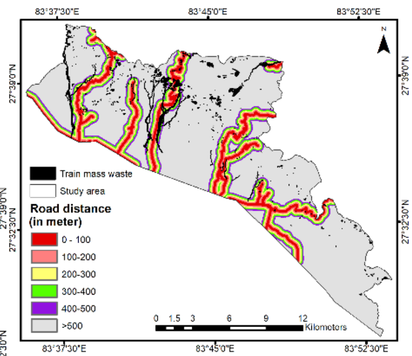

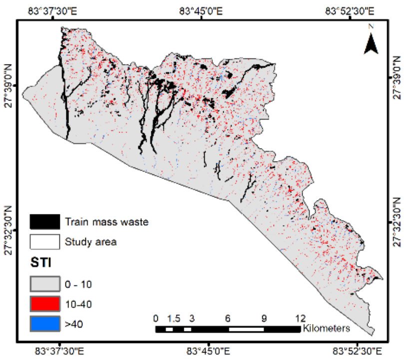

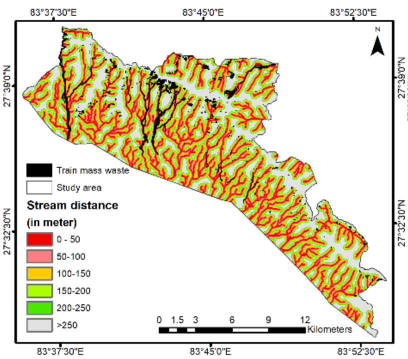

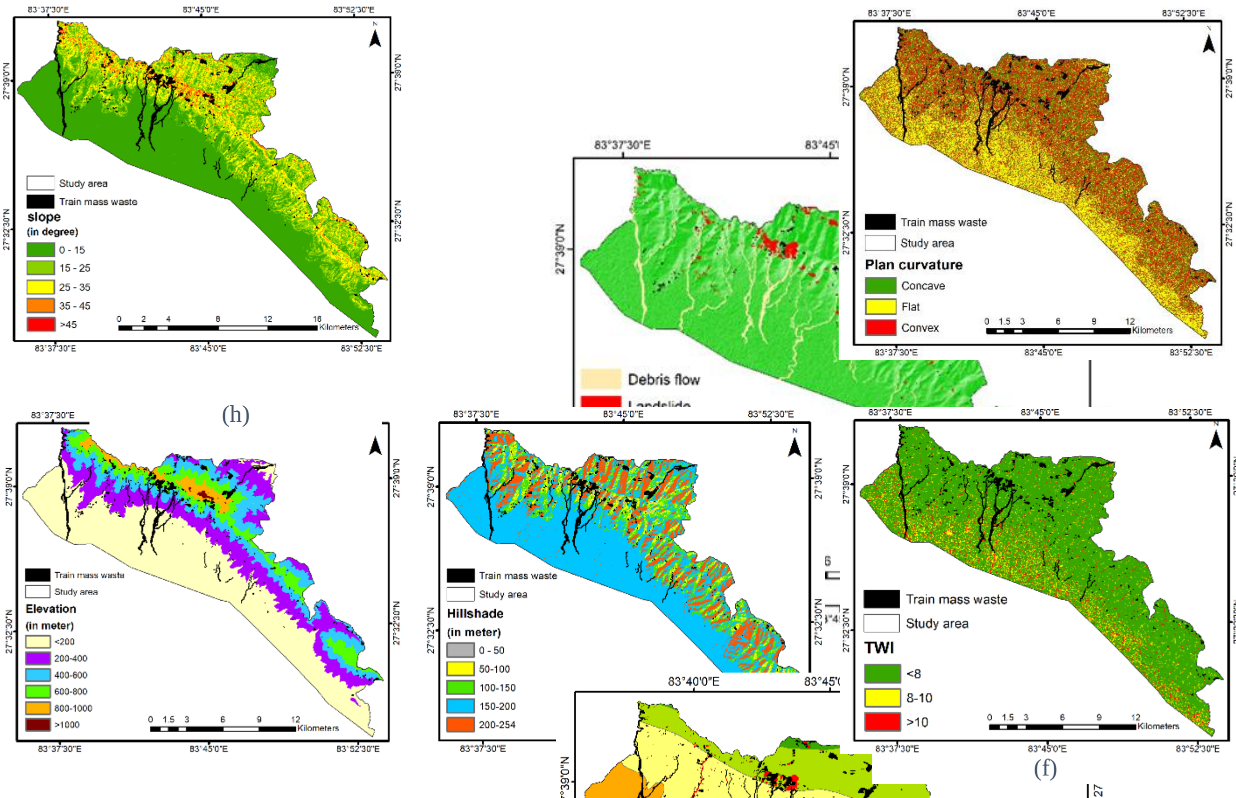

(h)

(f)

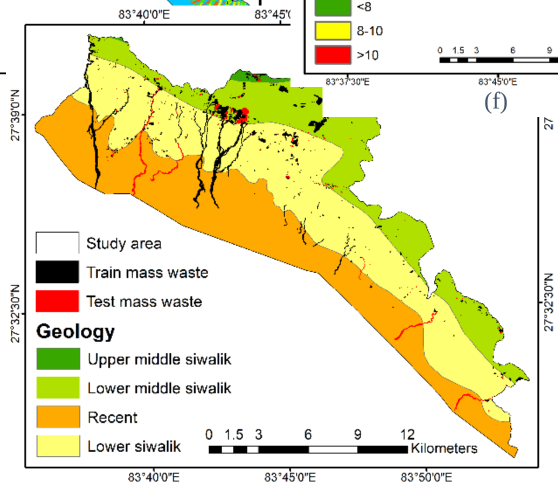

(k)

Figure 2: Geospatial factor maps (a) slope angle map; (b) slope aspect map; (c) curvature map; (d) elevation map; (e) Hillshade map; (f) TWI; (g)STI; (h) stream distance map; (i) road distance map; (j) geology map; (k) land use/land cover map

(g)

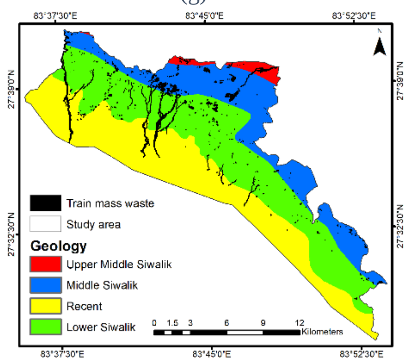

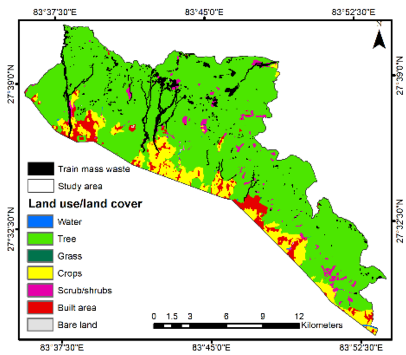

The ratio values acquired with FR were allocated as weight values to the classes of each component map to produce weighted factor thematic maps, which were then overlaid and numerically added with the raster calculator to produce the Mass-wasting Susceptibility Index map using Equation (4):

$$\text{Mass waste susceptibility index (MSI)} = \Sigma Fr \qquad (4)$$

Where Fr = the frequency ratio of each factor's range.

The calculated values of FR for each pixel in the susceptibility index indicate the relative susceptibility to mass waste occurrence. The higher pixel value of susceptibility index indicates higher susceptible to mass waste and the lower pixel value means the lower susceptible. Natural break method was applied to classify the mass waste susceptibility index. Using this method susceptibility index were classified into five classes i) Very low ii) Low iii) Medium iv) High v) Very high.

2.5 Validation

In the present study, the susceptibility maps were verified using the success rate and prediction rate curves to carry out a validation of the prediction results. For this, Susceptibility map was reclassified into 100 class in descending order. Then cross tabulate with train mass waste. From cross tabulation table success rate curve was obtained by plotting cumulative percentage area of train mass waste against cumulative percentage area of susceptibility map area. Similar procedure was applied to test mass waste to obtain prediction rate curve. Then accuracy assessment was carried out using area under curve (AUC) method (Kayastha et al., 2012; Regmi et al., 2014).

3 Results and Discussion

3.1 Mass-wasting Inventory Map

Mass-wasting inventory map were prepared using high resolution Google Earth images. Total 680 polygon of mass waste phenomena include Landslide (352 polygon), Debris flow channel (22 polygon) and Erosion (306 polygon) were recognized (Fig.3). Average length and width of landslide was found 126.68 m and 57.68m respectively. Similarly, average length and width of erosion was found 56.34 m & 28.92m. Average straight length of Debris flow channel was found 2578m.

Study showed that as Upper Middle Siwalik, Lower Middle Siwalik, Lower Siwalik and Recent geologic region had landslide density 3.32 per sq. km, 2.74 per sq. km, 1.77 per sq. km and 0.16 per sq. km respectively. Similarly, erosion density of respective class was found 0.87 per sq. km, 1.46 per sq. km, 1.97 per sq. km and 0.40 per sq. km respectively.

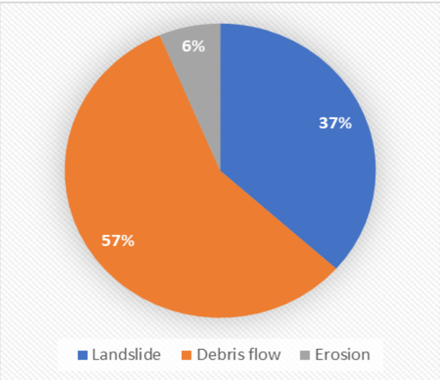

Figure 3: Mass-wasting inventory map

Study area cover 250 sq. km, out of which mass waste cover total 7.24 sq. km (2.89%). Landslide cover 2.65 sq. km, Debris flow cover 4.13 sq. km and Erosion cover 0.46 sq. km. Landslide, Debris flow and Erosion contributes 36.60%, 57.04% and 6.36% respectively to total mass waste phenomena (Fig.4). 35% of total mass waste occurs in Middle Siwalik (include both upper and lower middle siwalik) region. 33.52 % of total mass waste occurs in lower siwalik region while 31.48 % of total mass waste occurs in recent geological region.

3.2 Susceptibility mapping

Figure 4: Distribution of mass waste across geological region

Frequency ratio model was applied to prepare susceptibility map. Each factors map was reclassified and overlying with train mass waste. Cross tabulated data exported in Microsoft excel to analyze by frequency ratio approach. Frequency ratio for each factor classes were shown in (Table 1).

Table 1 shows at the slope gradient >25, frequency ratios were found >1. East, Southeast, South and Southwest aspect shows positive correlation with Mass-wasting phenomena occurrence while other aspect shows negative correlation. In case of curvature, only concave slope shows positive correlation (FR=1.18) with mass waste occurrence (Table 1). In the case of elevation, FR value higher than 1 is found at the elevation ranging from 400–1000 m classes. While other classes < 400m and > 1000 m were found <1 (Table 1). In the study area, relative relief was found to be varying between 0 to 254 m. FR value showed the higher correlation between mass waste occurrence and elevation from 0 to 100 m (Table 1). FR value increased with increasing TWI & STI value (Table 1). In the case of distance from stream, the distance in between 0 -100 m shows the highest correlation with the mass waste phenomena (Table 1). But in case of road distance, classes in between 100-500 m show positive correlation i.e. FR>1 while distance <100 m and >500m show FR<1 (Table 1). Upper Middle Siwalik (MS2) found to be highest frequency ratio value (2.25) followed by Lower Middle Siwalik (MS1) with frequency ratio value (1.41) (Table 1). From the frequency ratio analysis, Bare land was found most prone to the mass-wasting phenomena followed by water body. Scrub/shrub land cover also show positive correlation, but other land cover body did not show positive correlation with mass waste phenomena (Table 1).

Table 1: Mass-wasting conditioning factors and its frequency ratio values

Factors	Class	No. of pixels in class	Percentage of pixels in class	No. of pixels in mass waste	Percentage of pixels in mass waste	FR
Slope (degree)	<15	872704	54.607037	17065	50.8507405	0.9312
	15-25	381422	23.866426	3377	10.0628743	0.4216
	25-35	264262	16.535463	5635	16.7913227	1.0155
	35-45	70367	4.4030202	5134	15.2984296	3.4745
	>45	9398	0.5880538	2348	6.9966328	11.898
Aspect	North	124022	7.7603333	1695	5.05080604	0.6508
	Northeast	119005	7.4464084	1926	5.73914598	0.7707
	East	140262	8.7765064	3666	10.9240442	1.2447
	Southeast	221816	13.879522	6762	20.1495873	1.4517
	south	244404	15.292904	5635	16.7913227	1.098
	Southwest	290448	18.17398	6288	18.7371495	1.031
	West	234897	14.69803	4343	12.9413868	0.8805
	Northwest	167552	10.484103	2257	6.72546858	0.6415
	North	55747	3.4882142	987	2.94108883	0.8432
Plan Curvature	Concave	554083	34.506138	13779	40.9699096	1.1873
	Planar	480282	29.910098	8670	25.77902	0.8619

	Convex	571387	35.583764	11183	33.2510704	0.9344
Elevation (m)	<200	772211	48.090303	15271	45.4061608	0.9442
	200-400	346272	21.564476	4865	14.4653901	0.6708
	400-600	270057	16.818101	6700	19.9215033	1.1845
	600-800	163089	10.15655	5269	15.666627	1.5425
	800-1000	51069	3.180379	1492	4.43625119	1.3949
	>1000	3054	0.1901913	35	0.10406755	0.5472
Hillshade	0-50	23611	1.4807888	2848	8.49870192	5.7393
	50-100	100764	6.3195207	2873	8.57330429	1.3566
	100-150	242219	15.191021	4428	13.2135717	0.8698
	150-200	953601	59.806094	18746	55.9398406	0.9354
	200-254	274293	17.202575	4616	13.7745815	0.8007
TWI	<8	1362905	85.280008	27054	80.6162281	0.9453
	8-10	151236	9.4631741	3318	9.88706457	1.0448
	>10	84012	5.2568183	3187	9.49670729	1.8066
STI	0-10	1510456	94.512603	29274	87.2314431	0.923
	10-40	72624	4.5442458	3247	9.67549689	2.1292
	>40	15073	0.9431513	1038	3.09305998	3.2795
Stream distance (m)	0-50	294394	18.333647	13921	41.3921265	2.2577
	50-100	262088	16.321762	6055	18.003687	1.103
	100-150	228922	14.25632	3430	10.1986204	0.7154
	150-200	213508	13.2964	2829	8.41163178	0.6326
	200-250	178922	11.142526	2354	6.99928639	0.6282
	>250	427924	26.649346	5043	14.994648	0.5627
Road distance (m)	0-100	113068	7.0414097	1748	5.19743102	0.7381
	100-200	96042	5.9811005	2703	8.03698858	1.3437
	200-300	89348	5.5642257	2840	8.44433873	1.5176
	300-400	85760	5.3407799	2340	6.95765937	1.3027
	400-500	80510	5.0138315	2765	8.22133682	1.6397
	>500	1141030	71.058653	21236	63.1422455	0.8886
Geology	MS2	36635	2.2815111	1729	5.14200743	2.2538
	MS1	370699	23.085953	11005	32.7286245	1.4177
	Recent	570414	35.523567	9136	27.1702602	0.7649
	Lower Siwalik	627986	39.108968	11755	34.9591078	0.8939
Land cover	Water	3976	0.1584732	536	1.59334126	10.054
	Tree	2058377	82.041633	17616	52.3662307	0.6383
	Grass	518	0.0206462	0	0	0
	Crops	238527	9.5070751	1476	4.38763377	0.4615

	Scrub/Shrub s	79158	3.1550351	9226	27.4256837	8.6927
	Built up	119847	4.7767944	453	1.34661118	0.2819
	Bare land	8539	0.3403427	4333	12.8804994	37.846

Final susceptibility map obtained by FR model shown in (Fig 7). Susceptibility map was categorized into five classes. Higher the value of susceptibility index value greater is the susceptibility of the zone. Categorized result showed that as very low, low, medium, high and very high class covered 42.38%, 28.52%, 22.94%, 4.19% and 1.95% respectively of the total study area (Fig.5).

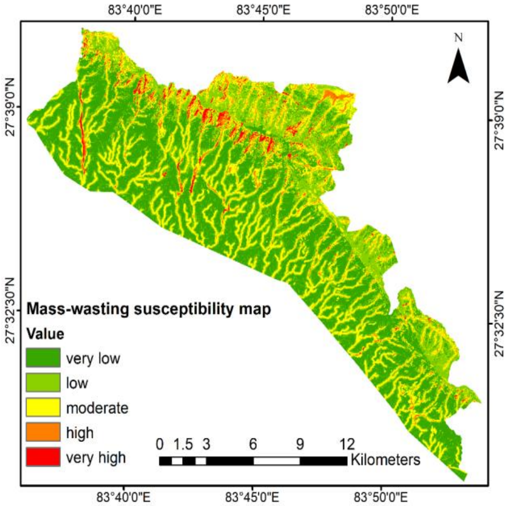

Figure 5: Mass waste susceptibility map

Performance of FR model was evaluated using area under curve (AUC). Success rate curve showed 82.15 % of the area lying under curve with train mass waste dataset. Similarly the prediction rate curve prepared using test mass waste (validation) dataset showed 78.30 % of the area lying under the curve indicating that prediction ability of the Frequency Ratio model (Fig. 6).

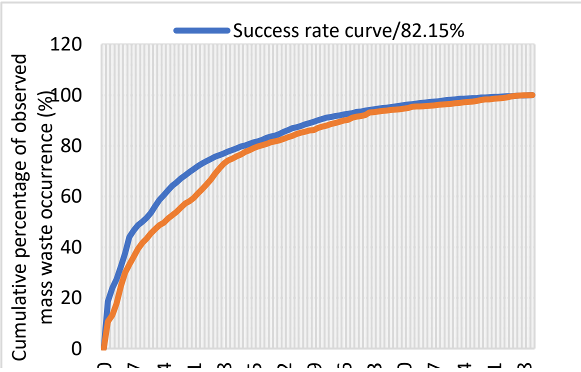

Figure 6: Validation Curve

3.3 Discussions

Mass-wasting susceptibility index map showed that very low, low, moderate, high and very high class cover 42.38%, 28.52%, 22.94%, 4.19% and 1.95% respectively of the total study area. It was observed that all eleven geospatial parameter strongly influencing the occurrence of the mass waste phenomena. Study showed mass waste occurrence (both in area and number) on land use and land cover type is very significant. Mostly Barren land cover was found to be highly susceptible to mass waste phenomena followed by water body and Scrub/shrubs land cover. This result agrees with that of Ghimire (2011)'s study.

(Bhandari & Dhakal, 2020a) suggest that the area and quantity of mass waste are bigger in Middle Siwalik, while medium to large mass waste are prominent in all formations. Our results showed highest quantity of mass waste (35% of total mass waste) occurs in middle siwalik region. Highest erosion density (1.97 per sq. km) was found in Lower Siwalik region because the Lower Siwaliks are mostly made up of weak mudstones that are easily weathered, and erosion is common (Dhakal, 2015). From the field investigation it was observed that Landslide occurrence increased with increasing slope while debris mass deposition decreased with increasing slope and erosion distributed irregularly along the slope distribution. Field observation was satisfied by frequency ratio analysis. A sediment load of fine to large size pebbles and cobbles is conveyed through the narrow valleys and deposited into riverbeds in the foothills and Terai due to the steep gradient and constrained channel, as well as the very limited flood plain in the upstream areas (Ghimire & Timalsina, 2020). More than 90% debris mass was found to be deposited in riverbeds in the foothills and recent geologic region of our study area. In the case of aspect East, Southeast, South and Southwest aspect shows positive correlation with Mass-wasting phenomena occurrence which was similar the result obtained in Mugling-Narayanghat road section (Devkota et al., 2012). In case of curvature, concave areas had a highest frequency ratio value (1.18). The reason for this is that after heavy rains, a concave slope holds more water and maintains it for longer, potentially leading to a slope failure and mass waste (Pradhan et al., 2010). In the case of elevation, 400–1000 m classes were found higher probable to mass waste phenomena. While other classes < 400m and > 1000 m were found less probable to mass waste phenomena (Table 1)

Distance from stream channel has a clear influence on mass-wasting phenomena, because at a distance of <100 m the frequency ratio values positively correlated, indicating a lower probability of mass-wasting phenomena occurrence further away from the streams. (Kayastha et al., 2012) concluded similar results in Tinau watershed, Nepal. Analysis from frequency ratio values shows that distance from road 100-500m had frequency ratio values greater than 1 (Table 1). However, frequency ratio values less than 1 found over the distance from road at 100m distance. Thus, road distance considered to be less significant in mass waste occurrence (Devkota et al., 2012). In case of TWI and STI, high concentration of debris mass deposition along the stream channel caused frequency ratio values increased with increasing TWI and STI values (Table 1).

By comparing existing landslide locations with landslide susceptibility maps, both success rate and prediction rate curves were employed for validation. The success rate and prediction rate curves were obtained by employing training dataset 75% (510 mass waste polygon) and the validation dataset 25% (170 mass waste polygon). In our study, the area under the curve showed the success rate of 82.15% and prediction rate of 78.30% for the frequency ratio model. The quantitative relationship between the AUC and the model prediction accuracy is classified into the grades: 50–60% is weak, 60-70% is moderate, 70-80% is good, 80-90% is very good, and 90–100% is excellent (Khosravi et al., 2016). In this study, the success rate curve shows very good result and prediction rate curve shows good predictive result. Thus, models employed for this study showed good accuracy in predicting the Mass-wasting susceptibility of the study area. Many researchers successfully used the success rate curve and predictive rate curve to validate the results of the frequency ratio model (Regmi et al., 2014; Pham et al., 2015; Acharya et al., 2017; Cao et al., 2019).

4. Conclusion

In this study, remote sensing, and geographic information systems (GIS) are employed to obtain Mass-wasting susceptibility index (MSI) map. Total 680 polygon of mass waste phenomena include Landslide (352 polygons), Debris flow channel (22 polygons) and Erosion (306 polygons) were recognized. Based on observed correlations between mass waste phenomena and variables, frequency ratio model was carried out for the susceptibility analysis of Siwalik region of 'Nawalparasi (Bardaghat Susta West). Mass-wasting susceptibility index map was categorized into five classes. Categorized result showed that as very low, low, medium, high and very high class covered 42.38%, 28.52%, 22.94%, 4.19% and 1.95% respectively of the total study area. Slope greater than 25º, East, Southeast, South and Southwest aspect, concave slope, Upper Middle Siwalik, Lower Middle Siwalik, bare land cover, elevation from 400-1000m, distance from stream channel less than 100m are more susceptible to mass waste occurrence.

In our study, the area under the curve showed the success rate of 82.15% and prediction rate of 78.30%. More than 82% success rates indicate that frequency ratio model is suitable model for the Mass-wasting susceptibility in the study area. These Mass-wasting susceptibility maps can be used as a planning tool by prioritizing areas for controlling the mass waste effects. Plantation programs can be specialized to susceptible area. District boundary has been selected for this study so that district individually can implement action plan may reduce coordination issues. Debris mass deposition is also included in mapping. It will help to solve the recurring flood disaster during monsoon season in lower lying area of 'Nawalparasi (Bardaghat Susta West), Nepal.

References

Acharya, T. D., Yang, I. T., & Lee, D. H. (2017). GIS-based landslide susceptibility mapping of Bhotang, Nepal using frequency ratio and statistical index methods. *한국측량학회지*, *35*(5), 357-364.

Akgun, A., Sezer, E. A., Nefeslioglu, H. A., Gokceoglu, C., & Pradhan, B. (2012). An easy-to-use MATLAB program (MamLand) for the assessment of landslide susceptibility using a Mamdani fuzzy algorithm. *Computers & Geosciences*, *38*(1), 23-34.

Auden, J.B., 1935. Traverses in the Himalaya. *Records of the Geological Survey of India* 69, 123-167.

Bashyal, S., & Sharma, S. (2020). Management of Degraded Chure Hills through Soil Conservation Management of Degraded Chure Hills through Soil Conservation Practices (A Case Study of Hariwan Municipality-1, Sarlahi District) Intern Investigator: (Issue September).

Bhandari, B. P., & Dhakal, S. (2018). Lithological Control on Landslide in the Babai Khola Watershed, Siwaliks Zone of Nepal. *American Journal of Earth Sciences*, 5(3), 54–64. http://www.openscienceonline.com/journal/ajes

Bhandari, B. P., & Dhakal, S. (2019a). Evolutional Characteristics of Debris Flow in the Siwalik Hills of Nepal. *International Journal of Geosciences*, 10(12), 1049–1067. https://doi.org/10.4236/ijg.2019.1012060

Bhandari, B. P., & Dhakal, S. (2019b). Topographical and geological factors on gully-type debris flow in Malai River catchment, Siwaliks, Nepal. *Journal of Nepal Geological Society*, 59, 89–94. https://doi.org/10.3126/jngs.v59i0.24994

Bhandari, B. P., & Dhakal, S. (2020a). Compositional analysis and phase relations of soil mass from the active landslides of Babai River watershed, Siwalik zone of Nepal. *Engineering Geology*, 278(October). https://doi.org/10.1016/j.enggeo.2020.105851

Bhandari, B. P., & Dhakal, S. (2020b). Spatio-temporal dynamics of landslides in the sedimentary terrain: a case of Siwalik zone of Babai watershed, Nepal. *SN Applied Sciences*, 2(5), 1–17. https://doi.org/10.1007/s42452-020-2628-0

Bhandari, B. P., & Dhakal, S. (2021). A multidisciplinary approach of landslide characterization: A case of the Siwalik zone of Nepal Himalaya. *Journal of Asian Earth Sciences*: X, 5, 100061. https://doi.org/10.1016/j.jaesx.2021.100061

Cao, C., Chen, J., Zhang, W., Xu, P., Zheng, L., & Zhu, C. (2019). Geospatial analysis of mass wasting susceptibility of four small catchments in mountainous area of miyun county, Beijing. *International Journal of Environmental Research and Public Health*, 16(15). https://doi.org/10.3390/ijerph16152801

Chaudhari, R. S. (1982). Petrology of the Siwalik Group of Nepal Himalaya. *Recent Researches in Himalaya*, 8, 424-466.

Dahal, R. K. (2017). Landslide hazard mapping in GIS. *Journal of Nepal Geological Society*, 53, 63–91. https://doi.org/10.3126/jngs.v53i0.23808

Dahal, R. K., Hasegawa, S., Masuda, T., & Yamanaka, M. (2006). Roadside Slope Failures in Nepal during Torrential Rainfall and their Mitigation Road construction practice in Nepal. *Proc. Interpaevent Int. Symp, Niijigata 2006, Disaster Mitigation of Debris Flow, Slope Failures and Landslides*, 503–514.

Devkota, K. C., Regmi, A. D., Pourghasemi, H. R., Yoshida, K., Pradhan, B., Ryu, I. C., Dhital, M.R., Althuwaynee, O. F. (2012). Landslide susceptibility mapping using certainty factor, index of entropy and logistic regression models in GIS and their comparison at Mugling–Narayanghat road section in Nepal Himalaya. *Natural Hazards, 65(1), 135–165.* doi:10.1007/s11069-012-0347-6

Dhakal, S., 2015. Evolution of Geomorphologic Hazards in Hindu Kush Himalaya, In: Shaw, R. & Nibanupudi, H.K (Eds.), *Mountain Hazards and Disaster Risk Reduction* (pp. 53-72), Springer Japan, DOI: 10.1007/978-4-431-55242-0_4.

Dhital, M. R. (2017). Geomorphic approach of controlling mass movements on Tama Koshi road in Central Nepal. *Lowland Technology International*, 18(4), 283–296. https://doi.org/10.0001/ialt_lti

El Morjani, Z.E.A., Ebener, S., Boos, J. , Ghaffer, E.A & Musani, A. (2007). Modelling the spatial distribution of five natural hazards in the context of the WHO/EMRO Atlas of Disaster Risk as a step towards the reduction of the health impact related to disasters. *International Journal of Health Geographics* **6**, 8 (2007). https://doi.org/10.1186/1476-072X-6-8

Fort, M., Cossart, E., & Arnaud-Fassetta, G. (2010). Hillslope-channel coupling in the Nepal Himalayas and threat to man-made structures: The middle Kali Gandaki valley. *Geomorphology*, 124(3–4), 178–199. https://doi.org/10.1016/j.geomorph.2010.09.010

Froude, M. J. & Petley, D. N. (2018). Global fatal landslide occurrence from 2004 to 2016. *Natural Hazards & Earth Systems Science* 18, 2161–2181

Ghimire, M. (2011). Landslide occurrence and its relation with terrain factors in the Siwalik Hills, Nepal: case study of susceptibility assessment in three basins. *Natural Hazards* 56, 299–320. https://doi.org/10.1007/s11069-010-9569-7

Ghimire, M., & Timalsina, N. (2020). Landslide Distribution and Processes in the Hills of Central Nepal: Geomorphic and Statistical Approach to Susceptibility Assessment. *Journal of Geoscience and Environment Protection*, *08*(12), 276–302. https://doi.org/10.4236/gep.2020.812017

Hagen, T., 1969. Report on the geological survey of Nepal Preliminary reconnaissance. *ZuÈrich MeÂmoires de la Societe HelveÂtique des Sciences Naturelles* LXXXVI/1, 185.

Gokceoglu, C., Sonmez, H., Nefeslioglu, H.A., Duman, T.Y., Can, T., (2005). The 17 March 2005 Kuzulu landslide (Sivas, Turkey) and landslide susceptibility map of its near vicinity. *Engineering Geology*, 81(1): 65-83. DOI: 10.1016/j.enggeo.2005.07.011

Kayastha, P., Dhital, M. R., & De Smedt, F. (2012). Landslide susceptibility mapping using the weight of evidence method in the Tinau watershed, Nepal. *Natural Hazards*, *63*(2), 479–498. https://doi.org/10.1007/s11069-012-0163-z

Khosravi, K.; Pourghasemi, H.R.; Chapi, K.; Bahri, M (2016). Flash flood susceptibility analysis and its mapping using different bivariate models in Iran: A comparison between Shannon’s entropy, statistical index, and weighting factor models. *Environmental Monitoring & Assessment*, 188, 656.

Lague, D., & Davy, P. (2003). Constraints on the long-term colluvial erosion law by analyzing slope-area relationships at various tectonic uplift rates in the Siwaliks Hills (Nepal). *Journal of Geophysical Research: Solid Earth*, 108(B2). https://doi.org/10.1029/2002jb001893

Larsen, M. C., & Parks, J. E. (1997). How wide is a road? The association of roads and mass-wasting in a forested montane environment. *Earth Surface Processes and Landforms: The Journal of the British Geomorphological Group*, *22*(9), 835-848.

Lee, S. and Pradhan, B. (2007). Landslide Hazard Mapping at Selangor, Malaysia Using Frequency Ratio and Logistic Regression Models. *Landslides*, 4, 33-41. https://doi.org/10.1007/s10346-006-0047-y

Pham, B.T., Tien Bui, D., Indra, P. and Dholakia, M.B. (2015) Landslide Susceptibility Assessment at a Part of Uttarakhand Himalaya, India Using GIS-Based Statistical Approach of Frequency Ratio Method. *International Journal of Engineering Research and Technology*, 4, 338-344. https://doi.org/10.17577/IJERTV4IS110285

Pradhan, B., Lee, S., & Buchroithner, M. F. (2010). Remote sensing and GIS-based landslide susceptibility analysis and its cross-validation in three test areas using a frequency ratio model. *Photogrammetrie, Fernerkundung, Geoinformation*, *2010*(1), 17–32. https://doi.org/10.1127/1432-8364/2010/0037

Regmi, A. D., Yoshida, K., Pourghasemi, H. R., Dhital, M. R., & Pradhan, B. (2014). Landslide susceptibility mapping along Bhalubang — Shiwapur area of mid-Western Nepal using frequency ratio and conditional probability models. *Journal of Mountain Science*, 11(5), 1266–1285. https://doi.org/10.1007/s11629-013-2847-6

Rowden, K. W., & Aly, M. H. (2018). A novel triggerless approach for mass wasting susceptibility modeling applied to the Boston Mountains of Arkansas, USA. *Natural Hazards*, *92*, 347-367.

Singh, B. K. (2010). Assessment of the upstream Churia Hills and downstream Terai plains linkage: An environmental services perspective. *Banko Janakari*, 20(1), 17–23.

TU-CDES (2016). Landslide Inventory Characterization and Engineering Design for Mitigation Works of Chure Area in Ten Districts. *Central Department of Environmental Science, Tribhuvan University and Government of Nepal, President Chure-Tarai Madhesh Conservation Development Board, Kathmandu*.

Upreti, B.N. (1999) An Overview of the Stratigraphy and Tectonics of the Nepal Himalaya. *Journal of Asian Earth Sciences*, 17, 577-606. https://doi.org/10.1016/S1367-9120(99)00047-4

Yalcin, A., Reis, S., Aydinoglu, A.C., Yomralioglu, T., (2011). A GIS-based comparative study of frequency ratio, analytical hierarchy process, bivariate statistics and logistics regression methods for landslide susceptibility mapping in Trabzon, NE Turkey. *Catena*, 85, 274–287.

Zinck, J. A., López, J., Metternicht, G. I., Shrestha, D. P., & Vázquez-Selem, L. (2001). Mapping and modelling mass movements and gullies in mountainous areas using remote sensing and GIS techniques. *International Journal of Applied Earth Observation and Geoinformation*, 3(1), 43-53.